



This item was submitted to Loughborough's Institutional Repository (<https://dspace.lboro.ac.uk/>) by the author and is made available under the following Creative Commons Licence conditions.



CC creative commons
COMMONS DEED

Attribution-NonCommercial-NoDerivs 2.5

You are free:

- to copy, distribute, display, and perform the work

Under the following conditions:

BY: **Attribution.** You must attribute the work in the manner specified by the author or licensor.

Noncommercial. You may not use this work for commercial purposes.

No Derivative Works. You may not alter, transform, or build upon this work.

- For any reuse or distribution, you must make clear to others the license terms of this work.
- Any of these conditions can be waived if you get permission from the copyright holder.

Your fair use and other rights are in no way affected by the above.

This is a human-readable summary of the [Legal Code \(the full license\)](#).

[Disclaimer](#) 

For the full text of this licence, please go to:
<http://creativecommons.org/licenses/by-nc-nd/2.5/>

EVIDENCE FOR SWELLING-INDUCED PORE STRUCTURE IN DENSE PDMS NANOFILTRATION MEMBRANES

J.P. Robinson^a, E.S. Tarleton^a (e.s.tarleton@lboro.ac.uk), C.R. Millington^b and A. Nijmeijer^c

^aAdvanced Separation Technologies Group, Department of Chemical Engineering, Loughborough University, Loughborough, Leicestershire LE11 3TU, UK.

^bShell Global Solutions, Cheshire Innovation Park, P.O. Box 1, Chester CH1 3SH, UK.

^cShell Global Solutions International BV, P.O. Box 38000, 1030 BN Amsterdam, The Netherlands.

ABSTRACT

A dense polydimethylsiloxane (PDMS) membrane was used to assess the flux and separation performance of a range of solutes (e.g. poly-nuclear aromatics and organometallics) and organic solvents (e.g. heptane and xylene). Solvent flux was modelled with the Hagen-Poiseuille equation and found to fit the model well, with the degree of swelling influencing the effective pore size and porosity of the membrane.

The rejection mechanism for low-polarity solutes was found to be predominantly size exclusion. The rejection varied with solvent type and rejections were higher in poorer-swelling solvents. For instance, the rejection of 9,10 Diphenylanthracene was 2% in a pure heptane solvent compared with 15% in xylene. It is postulated that dense PDMS membranes exhibit the characteristics of a porous structure when swollen with solvent, and that the degree of swelling impacts on the separation performance of the membrane. A comparison between the Hildebrand solubility parameters for the PDMS membrane and the challenge solvent was found to be a good indicator of flux/rejection performance.

KEYWORDS

Nanofiltration; Membrane; PDMS; Non-aqueous; Solute rejection; Polymer swelling

INTRODUCTION

Nanofiltration (NF) is a process largely associated with aqueous systems such as the purification of drinking water. In recent times the feasibility of using polymeric NF membranes for non-aqueous systems has been explored, examples include the recovery of organometallic catalysts from organic solvents¹ and the de-acidification of vegetable oils². The initial development of thermodynamic theories was carried out by Paul and Ebra-Lima³ as early as 1970 whilst studies into polymer-solvent interactions were documented by Flory⁴ in the 1950s and since by others^{5,6}. Newer work has attempted to enhance the understanding of both hydraulic (physical) and chemical transport mechanisms as well as solute rejection.

When hydraulic transport is the predominant mechanism, viscous liquid flow through a membrane (and other porous media) is pressure dependent and described by the Hagen-Poiseuille equation:

$$J = \left(\begin{matrix} \text{membrane} \\ \text{properties} \end{matrix} \right) \left(\begin{matrix} \text{system} \\ \text{parameters} \end{matrix} \right) = \left(\frac{\epsilon r^2}{8LT} \right) \left(\frac{\Delta P}{\mu} \right) \quad (1)$$

where J is the flux, ϵ the porosity, r the average pore radius, ΔP the differential pressure across the membrane, μ the liquid viscosity, L the membrane thickness and τ the tortuosity factor. Equation (1) can be sub-divided into membrane properties (porosity, membrane thickness etc) and system parameters (pressure and viscosity). Under the viscous flow regime liquid mixtures will not

undergo separation unless there are significant interactions between a particular component and the membrane. In the wider context, Zwijnenberg *et al.*² demonstrate the importance of surface energy for both polar and non-polar solvents with hydrophilic membranes. Permeation through membrane pores is shown to be possible only when the difference in surface energy can be overcome by the applied pressure. Bhanushali *et al.*⁷ have also shown that solvent surface tension is inversely proportional to flux for hydrophobic membranes as the polarity of organic solvents is strongly related to surface tension.

With chemical transport, the solution-diffusion concept first proposed by Lonsdale *et al.*⁸ is favoured. The passage of a substance occurs via a dissolution-diffusion mechanism such that the separation potential is determined by differences in solubility and diffusivity⁹; the sorption process generally being non-ideal^{10,11}. A worthy alternative approach is the pore-flow model, where even the densest membrane is modelled as a porous structure through which solvent transport takes place. The Hildebrand solubility parameter, δ , is one method of estimating solvent affinity for a particular polymer¹². The parameter takes into account hydrogen-bonding, polar and dispersive effects, and can be assigned to both solvents and polymers from their molecular structures and chemical groups. Solvents and polymers that exhibit similar values of Hildebrand parameter are expected to interact strongly to give high solubility of the solvent in the polymer and hence significant polymer swelling. Such concepts have been assessed by Bhanushali *et al.*⁷ who found that solvents with $\delta \approx 15.5 \text{ MPa}^{0.5}$ cause PDMS membranes, which have a similar value of δ , to swell the most, with a maximum solubility of ~ 2 g solvent per g of polymer.

The rejection of organic solutes from organic solvents with polymer membranes has been addressed by relatively few workers. Scarpello *et al.*¹ studied organometallic solutes in a range of solvents with an MPF-50 membrane similar to PDMS and found that rejection increased with pressure, a phenomenon predicted by the solution-diffusion model. Gibbins *et al.*¹³ also report an increase in rejection with pressure, and found that rejection increased with solute molecular weight. The results of Gibbins favour the pore-flow model, as their measured solute flux was $\times 1000$ that predicted by the solution-diffusion model. Yang *et al.*¹⁴ in a study with aromatic dyes found rejection to vary according to the solvent used, and that the manufacturer specified molecular weight cut-off (MWCO) determined for the membrane with aqueous media is not valid for organic solvents. Increasing rejection with pressure and molecular weight, and solvent-specific rejections were also reported by van der Bruggen *et al.*¹⁵ and Koops *et al.*¹⁶, the latter employed cellulose-acetate membranes rather than the silicon-based membranes studied by other workers.

In conclusion, whilst some workers have found rejection data to be in agreement with the solution-diffusion model, others studying similar systems have found the pore-flow model to be a better descriptor. It is possible that a transitional mechanism exists in non-aqueous NF systems. In the current study a range of solutes in non-polar solvents have been used to investigate flow/rejection behaviour with the aim of clarifying understanding.

EXPERIMENTAL PROPERTIES AND PROCEDURES

Membrane

PAN (Polyacrylonitrile)/PDMS composite membranes with a nominal PDMS thickness of $2 \mu\text{m}$ were used for the study (see Figure 1 and Table 1). When received, the N_2 permeability was checked and found to be 280 ± 10 barrer assuming the nominal $2 \mu\text{m}$ thickness to be representative. An O_2/N_2 selectivity of 2.2 has previously been reported for the membrane¹⁷ and data related to O_2/N_2 selectivity and pure nitrogen permeation verify that the selective layer in the membrane is PDMS¹⁸.

Solvents and Solutes

Alkane and aromatic solvents, and organometallic and poly-nuclear aromatic (PNA) solutes, were chosen to be representative of those found in the industrial processes of interest. n-hexane, n-heptane, cyclohexane and xylene were obtained from Sigma-Aldrich Ltd. Branched isomeric alkanes, i-hexane, i-heptane and i-octane were supplied by Shell Global Solutions. Solute compounds were obtained from Sigma-Aldrich, Fisher Scientific and Strem Chemicals and selected on the basis of their solubility, molecular weight and abundance. A further (secondary) criteria was the ease with which their concentration in a particular solvent could be determined using spectrometric techniques. The chemical structures of the chosen solutes are shown in Figure 2 and other relevant data are presented in Table 2.

Apparatus

A schematic of the membrane module is shown in Figure 3. The module comprised two stainless steel discs, each of 150 mm diameter and 20 mm thickness. The bottom plate was milled to accommodate a 75 mm diameter sintered plate that fitted flush with its top surface. The flat-sheet membrane was cut into a 95 mm disc and positioned upon the sintered plate. A 3 mm thick PTFE gasket was placed over the top to clamp the membrane in position, produce a hydraulic seal and provide a space between the membrane and top plate that was subsequently filled with the solvent/solute combination. Inlet/outlet channels on the top plate allowed the module to operate in either a deadend or crossflow configuration.

When assembled, the membrane module was connected to a compressed nitrogen supply through a reservoir containing the feed solution. To progress a separation, the reservoir was raised to a known and constant pressure to promote liquid flow (via a dip-tube) into the membrane module. Crossflow rate was controlled by adjusting the valve on the retentate outlet of the membrane module. The permeate and retentate were kept separate throughout an individual experiment.

Experimental Methods

Pure solvent flux was measured in the deadend mode of operation, with two membrane samples being used to perform all experiments. Before commencing permeation experiments, the valve on the membrane module outlet was opened fully, and a small pressure applied to the fluid in the reservoir to bleed any excess air from the system. 100 ml of solvent was then run through the membrane module to remove any remaining gas and flush away any residual solvent from the previous test. The module exit valve was subsequently closed, and the pressure increased to the test pressure. The permeate was left to drain for 10 mins. to establish a steady-state before being collected in a narrow-necked flask. Experiment duration was sufficient to allow approximately 100 ml of solvent to permeate the membrane. Permeation rate was determined by weighing the collected permeate at specified time intervals.

Solute rejection experiments were performed using a similar general approach. However, in this case the module exit valve was opened to permit a small crossflow ($\sim 20 \text{ ml min}^{-1}$) and stop the undesirable build-up of solute within the immediate vicinity of the membrane surface. Crossflow rate was adjusted to achieve a stage-cut of 20–25%. Rejection data were obtained with n-heptane and xylene, representative of alkane and aromatic solvents respectively. Solute was added to a solvent within the concentration range 10–25 ppm by weight, this being representative of that found in the industrial processes to which this study is related. The level of rejection was determined using a Lambda 12 UV/vis spectrometer. Calibration was carried out at several wavelengths for a given solute in each solvent, the absorbance-concentration profile being linear in each case. Typical minimum detection levels for the solute compounds were in the order of 100 ppb.

RESULTS AND DISCUSSION

The results presented in Table 1 and Figures 4-6 summarise the data obtained for the range of solvents, solutes and operating conditions described. They are a representative of the complete data set obtained.

Repeatability

The solvent fluxes reported were obtained using two samples of PDMS membrane. As a consequence of manufacturing variances, the flux between different membrane samples could vary by up to $\pm 10\%$. Flux through individual membranes could vary by $\pm 2\%$ over a period of several days. Whether a membrane was stored in a swollen-state or allowed to dry had no apparent impact on the flux or separation performance.

In order to account for the slight variability between different membranes and the small flux increase with time, the flux-pressure relationship for n-heptane was determined initially. n-heptane fluxes were also measured at 300, 600 and 900 kPa before the flux-pressure relationship of a new solvent was determined. The ratio of (solvent flux) to (n-heptane flux) was calculated in each series of experiments and that ratio used to calculate the solvent flux based on the original n-heptane data. The re-calculated values enabled solvent fluxes to be accurately compared.

No attempt was made to adjust the measured solute rejections based on the rejection of a standard solute compound. The validity of the solute rejection data was confirmed in each experiment by applying a mass balance that was generally found to be within 1%.

Flux and Rejection Measurements

The flux behaviour of pure organic solvents with the PDMS polymer membrane are shown in Table 1, and comparisons with the Hagen-Poiseuille model described by Equation (1) are shown in Figure 4. For the chosen solvents, the data fall on three distinct regression lines that correlate well with the different classifications of solvent. The divisions of gradient show that solvent groups affect their own membrane properties (i.e. values of $\epsilon^2/(8L\tau)$) whilst individual items within a classification produce similar degrees of swelling. Although one of several parameters could potentially be altered, the (effective) pore radius, r , is most likely to be influenced by the solvent/polymer combination. When swollen, it seems that the structure of the dense PDMS layer changes to become porous and allow viscous flow to a level partly dependent on the swelling properties of the solvent.

Comparisons of the data in Figure 4 and Tables 1 and 2 show that the flux levels for the cyclic compounds are above those that could be expected from superficial comparisons of solubility parameters. It is also notable on Table 1 and Figure 4 that the data correlations have a significant positive intercept when extrapolated to the y-axis. Further experiments (not reported here) show that two distinct regions in the flux-pressure relationship can exist for solvents. Possible reasons include the linear and reversible compaction of the PDMS layer at pressures up to ~ 200 kPa and/or a small, but finite, contribution to transport from chemical mechanisms¹⁹. It is also possible that molecule shape may influence the permeation process (see later).

When a mixture of alkane and aromatic solvent was permeated through a membrane sample, no separation was noted within the resolution of the refractometry detection technique. This again points to a viscous flow regime and a porous membrane structure. If a chemical transport mechanism was significant then a separation of components would be expected due to differences in diffusion rates. Similar results have been reported by Machado *et al.*²⁰ for a range of solvent mixtures with silicon-based MPF-50 membranes.

The influence of swelling on flux was emphasised by experiments with water (a polar solvent). Referring to Table 2, the viscosity of water is similar to that of cyclohexane. Thus, for a constant membrane porosity/pore size and a simple hydraulic transport mechanism, the rate of water

permeation should be close to that recorded with cyclohexane. Permeation tests with the PDMS membrane indicated zero water flux up to the maximum system pressure of 900 kPa, a result that has been confirmed by other workers for both PDMS and MPF-50 membranes^{11,15}. As water exhibits a high solubility parameter ($\delta = 47.5 \text{ MPa}^{0.5}$) due to its polar nature it does not induce any appreciable swelling of the hydrophobic PDMS layer ($\delta = 15.5 \text{ MPa}^{0.5}$) and the membrane remains in its dense state to prevent water permeation.

In experiments with another polar solvent, pure ethanol ($\delta = 26.2 \text{ MPa}^{0.5}$), the permeation rate through the membrane was measured at approximately two orders of magnitude below that for n-heptane ($\delta = 15.3 \text{ MPa}^{0.5}$). From these data, and in the absence of PDMS swelling, it is reasonable to expect a 50% ethanol/n-heptane mixture to yield an ethanol rejection >90%. Such a mixture was permeated through a membrane at a pressure of 600 kPa and a crossflow rate of 20 ml min^{-1} to produce an ethanol rejection of ~5%. The behaviour can again be explained by swelling induced porosity of the PDMS layer. A comparison of solubility parameters (Table 1) shows ethanol to be a poor swelling solvent for PDMS. However, n-heptane has a solubility parameter close to that of PDMS and is a very good swelling solvent for the active membrane layer. With a binary mixture such as ethanol/n-heptane, it is considered that n-heptane swells the dense PDMS sufficiently to induce porosity and allow significant ethanol permeation through the membrane.

If PDMS is porous in the swollen state then the rejection of low-polarity, minimally interacting, solutes in good swelling solvents should be predominantly via a size-exclusion mechanism. To assess this possibility, the rejection behaviour of organic solute compounds with a range of molecular weights was determined in a xylene solvent ($\delta = 18.2 \text{ MPa}^{0.5}$) at pressures of 600 kPa (see Figure 5). From the data obtained the membrane appears to have a MWCO in the region of 400 g mol^{-1} . Increasing solute rejection with molecular weight has been reported by Gibbins *et al.*¹³ for an MPF-50 membrane; here, solute molecular weights ranged from 250 to 400 g mol^{-1} . A size-exclusion mechanism is unlikely for dense membranes as solute transport is diffusive in nature. Although larger molecules can be expected to have very low rates of diffusion through dense membranes and thus high rejections, smaller molecules would not be expected to give zero rejections as observed in Figure 5. The latter could potentially occur through one of three scenarios:

- Solvent is transported via viscous flow and solute flux is diffusive. For this scenario to occur the solvent and solute fluxes would need to be identical.
- Solvent and solute fluxes both occur via a diffusive mechanism at identical rates.
- Solvent and solute are transported via a viscous flow mechanism at the same rate.

In the authors opinion, the most feasible explanation is the third scenario where the solvent swells the membrane sufficiently to induce a porous structure, and the zero rejections are due to the solvent and solute moving through the membrane structure 'as one' under viscous flow with no separation occurring. Zero rejections have previously been reported by van der Bruggen *et al.*¹⁵, who studied the rejection behaviour of a solute with a molecular weight of 340 g mol^{-1} in a range of solvents with an MPF-50 membrane. They found that solute rejection was zero in n-hexane, and suggest that contact with organic solvents increases the mobility of the polymeric chains in the membrane, allowing unhindered transport of solvent and solute.

Should a membrane become porous when swollen then the degree of swelling will affect the porosity and effective pore size of the membrane with a subsequent impact on separation performance. The data in Figures 4 and 5 support the idea that good swelling solvents affect a larger porosity and pore size than poor swelling solvents, resulting in lower solute rejections. Whilst a comprehensive study of rejection in different solvents is beyond the scope of the current work, rejections of identical solutes have been compared in cyclic (xylene, $\delta = 18.2 \text{ MPa}^{0.5}$) and straight chain (n-heptane, $\delta = 15.3 \text{ MPa}^{0.5}$) solvents. Based on the solubility parameters and data reported by Bhanushali *et al.*⁷, n-heptane swells PDMS more than xylene and hence the rejection

of low-polarity solute compounds is expected to be higher in xylene than n-heptane. Figure 6 shows rejections of three solute compounds at concentrations of 20 ppm in n-heptane and xylene solvents; pressure and crossflow were maintained at 600 kPa and 20 ml min⁻¹ respectively. The data indicate that the rejection of identical solute compounds is higher in the poorer-swelling xylene solvent, which is consistent with the proposed hypothesis. Other data (Table 1) show a corresponding increase in the flux level for the better swelling solvent. It is postulated that the increased swelling caused by n-heptane raises the effective pore size and porosity of the membrane which in turn improves the physical transport of the solute molecules, leading to a lower rejection. The results of Scapello *et al.*¹ and van der Bruggen *et al.*¹⁵ who studied solute rejection in different solvents with an MPF-50 membrane do not confirm such an effect, although a direct comparison is not possible due to the polar nature of the solvents and solutes used in their work. Polar solutes are likely to interact with the hydrophobic membrane surface, resulting in rejection mechanisms different from the size-exclusion mechanism identified in this work. Similarly, polar solvents are likely to interact with both polar solute compounds and the membrane surface, which makes the comparison with a size-exclusion mechanism very difficult.

An estimation of the effective pore radius of the swollen membrane can be determined from the pore model first proposed by Ferry²¹. The model is able to predict pore radii based on the radius of a solute molecule and its corresponding rejection by assuming the membrane to comprise cylindrical pores. For 9,10 Diphenylanthracene, an equivalent solute radius of 0.71 nm was calculated from covalent radii and bond lengths within the molecule. For the 9,10 Diphenylanthracene rejections shown in Figure 6, the pore radius in a xylene solvent is calculated as 1.88 nm, compared with 1.98 nm in n-heptane. By way of comparison the steric hindrance pore model²² gives pore radii of 3.23 nm in xylene and 7.97 nm in n-heptane. Assuming the models to be valid, the predicted pore radii give an indication of the order of magnitude of the pore size in swollen PDMS membranes. For the 9,10 Diphenylanthracene solute, a comparison of the calculated molecule and membrane pore radii supports the relatively poor rejection noted.

Solvent and Solute Molecule Shape

Some of the data noted in Figures 4-6 could be affected by the inherent shapes of the solvent and solute molecules.

The different gradients for the three solvent classifications in Figure 4 may be influenced by steric effects. Referring to Figure 2, the cyclic nature of cyclohexane and xylene is likely to yield more rigid molecules than n- and i-alkanes, and thus reduce their tendency to compress when under pressure. Compressibility effects will cause the solvent viscosity to increase as the molecules become more ordered, and could influence the distinct correlations identified in Figure 4. Viscosity increases will only be prevalent in flow through porous membranes; Bowen and Welfoot²³ have considered such an effect with nanofiltration membranes and aqueous feeds.

Similar data to that presented in Figure 5 have been obtained for a non-cyclic solvent. When tested in n-heptane, Copper (II) naphthenate gave a rejection of only 90% despite having the largest average molecular weight (611 g mol⁻¹) of all the compounds studied. Iron (III) naphthenate has a lower average molecular weight (448 g mol⁻¹) and yet gave a higher rejection of 96%. Such behaviour may potentially be explained by considering the shape of the two naphthenate compounds. Iron (III) naphthenate has a trigonal-planar structure due to the three naphthenic acid groups coordinating with the Fe molecule. Copper (II) naphthenate is linear and individual molecules, despite their large size, may be able to orientate themselves such that they are able to pass through a porous structure at a greater rate than Iron (III) naphthenate.

CONCLUSIONS

Although the available data are not yet sufficient to test the relative merits of the pore-flow and solution-diffusion models, this study presents significant evidence to show that PDMS membranes exhibit the characteristics of a porous structure when swollen with a suitable solvent. Good agreement with the Hagen-Poiseuille model and the non-separation of binary solvent mixtures shows that viscous flow occurs through the membrane. The concept of viscous flow is also supported by the observation that the rejection mechanism for non-polar solutes is predominantly one of size exclusion. The low permeation rate of pure ethanol compared with the much higher value when mixed with n-heptane shows that increased membrane swelling improves the transport of polar substances that exhibit a high solubility parameter. Poor-swelling solvents yield a lower flux and higher solute rejection than good-swelling solvents. It is postulated that swelling increases the effective pore size and porosity of the membrane and that the Hildebrand solubility parameter is a good indicator of swelling potential for solutes in non-polar solvents with a PDMS membrane as well as a good predictor of their subsequent flux/rejection behaviour.

ACKNOWLEDGEMENTS

Shell Global Solutions (UK) are acknowledged for supplying project funding, technical hardware and isomeric solvents. EPSRC are also acknowledged for part-funding the project from which the presented work is taken. The PDMS membranes were kindly supplied by GKSS Forschungszentrum.

NOMENCLATURE

J	solvent flux ($\text{l m}^{-2} \text{h}^{-1}$)
L	membrane thickness (m)
ΔP	differential pressure (Pa)
r	pore radius (m)
δ	Hildebrand solubility parameter ($\text{MPa}^{0.5}$)
ε	porosity
μ	viscosity (Pa s)
τ	tortuosity factor

barrer $\times 10^{-10} \text{ cm}^3(\text{STP}).\text{cm cm}^{-2} \text{ s}^{-1} (\text{cm.Hg})^{-1}$

REFERENCES

1. Scarpello J.T., Nair D., Freitas dos Santos L.M., White L.S. and Livingston A.G., 2002, The separation of homogeneous organometallic catalysts using solvent resistant nanofiltration, *J. Membrane Science*, **203**, 71-85.
2. Zwijnenberg H.J., Krosse A.M., Ebert K., Peinemann K-V. and Cuperus F.P., 1999, Acetone-stable nanofiltration membranes in deacidifying vegetable oil, *J. American Oil Chemists Society*, **76**, 83-87.
3. Paul D.R. and Ebra-Lima O.M., 1970, Pressure-induced diffusion of organic liquids through highly swollen polymer membranes, *J. Applied Polymer Science*, **14**, 2201-2224.
4. Flory P.J., 1953, *Principles of Polymer Chemistry*, Cornell University Press, Ithaca, NY.
5. Sun Y.-M. and Chen J., 1994, Sorption/desorption properties of ethanol, toluene and xylene in poly (dimethylsiloxane) membranes, *J. Applied Polymer Science*, **51**, 1797-1804.

6. Yoo J.S., Kim S.J. and J.S. Choi., 1999, Swelling equilibria of mixed solvent/poly (dimethylsiloxane) systems, *J. Chemical Engineering Data*, **44**, 16-22.
7. Bhanushali D., Kloos S., Kurth C. and Bhattacharyya D., 2001, Performance of solvent-resistant membranes for non-aqueous systems: solvent permeation results and modelling, *J. Membrane Science*, **189**, 1-21.
8. Lonsdale H., Merten U. and Riley R., 1965, Transport of cellulose acetate osmotic membranes, *J. Applied Polymer Science*, **9**, 1341-1362.
9. Wijmans J.G. and Baker R.W., 1995, The solution-diffusion model: A review, *J. Membrane Science*, **107**, 1-21.
10. Sun Y-M. and Chen J., 1994, Sorption/desorption properties of ethanol, toluene and xylene in poly(dimethylsiloxane) membranes, *J. Applied Polymer Science*, **51**, 1797-1804.
11. Favre E., Schaezel P., Nguyen Q.T., Clement R. and Neel J., 1994, Sorption, diffusion and vapour permeation of various penetrants through dense poly (dimethylsiloxane) membranes: a transport analysis, *J. Membrane Science*, **92**, 169-184.
12. Barton A.F.M., 1983, *CRC Handbook of Solubility Parameters and Other Cohesion Parameters*, CRC Press, London.
13. Gibbins E., D'Antonio M., Nair D., White L.S., Freitas dos Santos L.M., Vankelecom I.F.J. and Livingston A.G., 2002, Observations on solvent flux and solute rejection across solvent resistant nanofiltration membranes, *Desalination*, **147**, 307-313.
14. Yang X.J., Livingston A.G. and Freitas dos Santos L., 2001, Experimental observations of nanofiltration with organic solvents, *J. Membrane Science*, **190**, 45-55.
15. van der Bruggen B., Geens J. and Vandecasteele C., 2002, Fluxes and rejections for nanofiltration with solvent stable polymeric membranes in water, ethanol and n-hexane, *Chemical Engineering Science*, **57**, 2511-2518.
16. Koops G.H., Yamada S. and Nakao S.-I., 2001, Separation of linear hydrocarbons and carboxylic acids from ethanol and hexane solutions by reverse osmosis, *J. Membrane Science*, **189**, 241-254.
17. GKSS Forschungszentrum. *Technical Datasheet*. October 2001.
18. Mulder M.H.V., 1991, *Basic Principles of Membrane Technology*, Kluwer Academic Publishers, Dordrecht.
19. Robinson J.P., Tarleton E.S., Millington C.R. and Nijmeijer A., 2004, Solvent flux through dense polymeric nanofiltration membranes, *J. Membrane Science*, **230**, 29-37.
20. Machado D.R., Hasson D. and Semiat R., 1999, Effect of solvent properties on permeate flow through nanofiltration membranes. Part 1: Investigation of parameters affecting solvent flux, *J. Membrane Science*, **163**, 93-102.
21. Ferry J.D., 1936, Statistical evaluation of sieve constants in ultrafiltration, *J. General Physiology*, **20**, 95-104.

22. van der Bruggen B., Schaep J., Wilms D. and Vandecasteele C., 2000, A comparison of models to describe the maximal retention of organic molecules in nanofiltration, *Separation Science Technology*, **35**(2), 169-182.
23. Bowen W.R. and Welfoot J.S., 2002, Modelling the performance of membrane nanofiltration – critical assessment and model development, *Chemical Engineering Science*, **57**, 1121-1137.

FIGURES AND TABLES

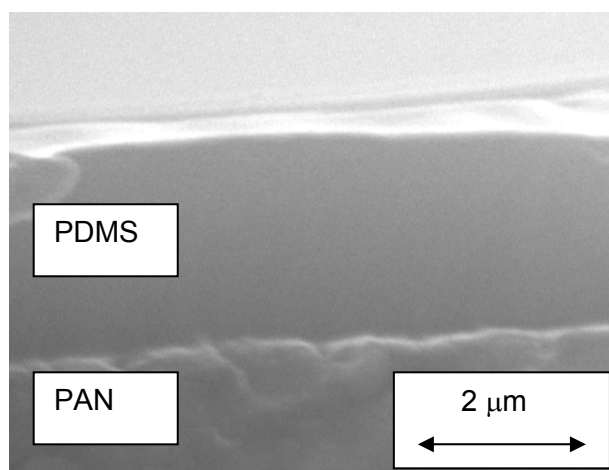


Figure 1: Freeze fractured membrane cross-section showing a nominal 2 μm PDMS layer on the PAN (Polyacrylonitrile) substrate - measured layer thickness could vary between 1.5 and 3 μm for different membrane samples.

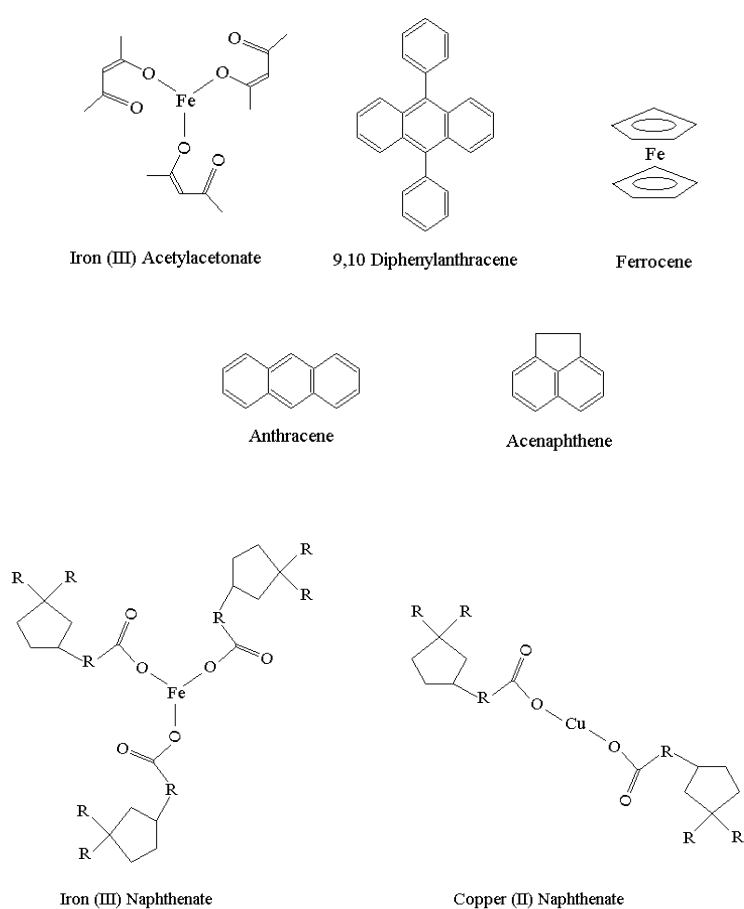


Figure 2: Structures of the chosen solute compounds, R denotes alkyl groups.

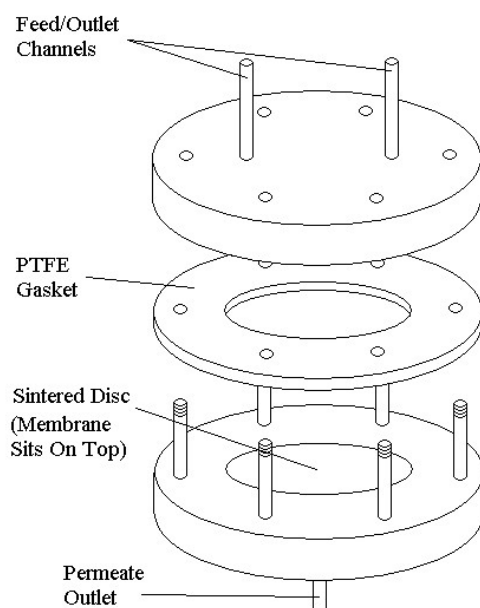


Figure 3: Schematic of the flat-sheet membrane module.

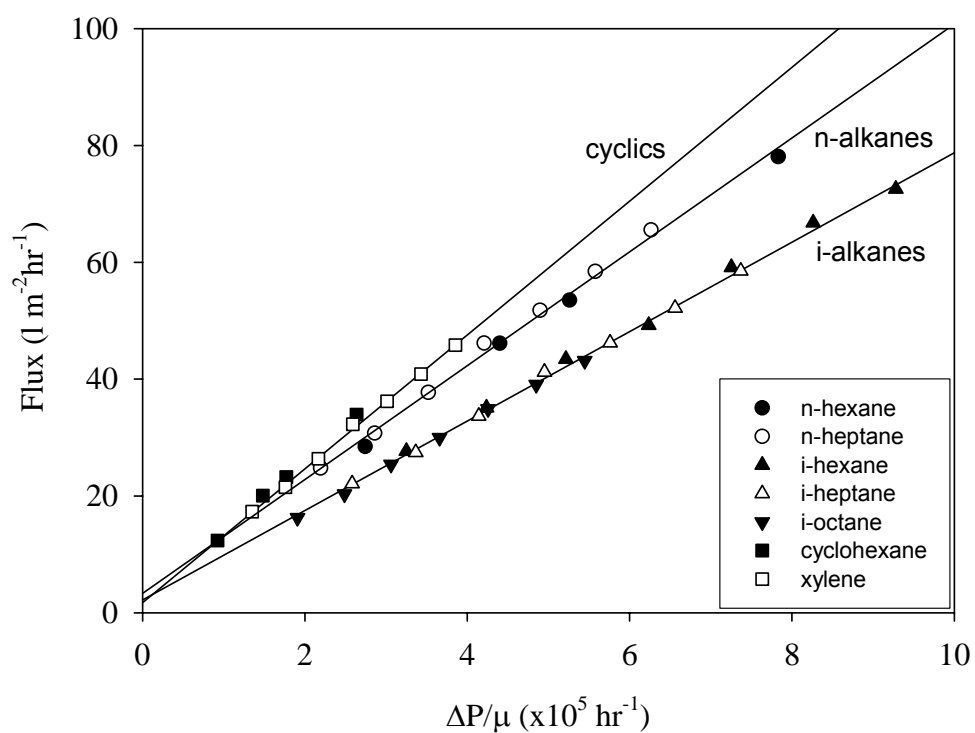


Figure 4: Hagen-Poiseuille plot for a range of organic solvents (viscosity values at 20°C).

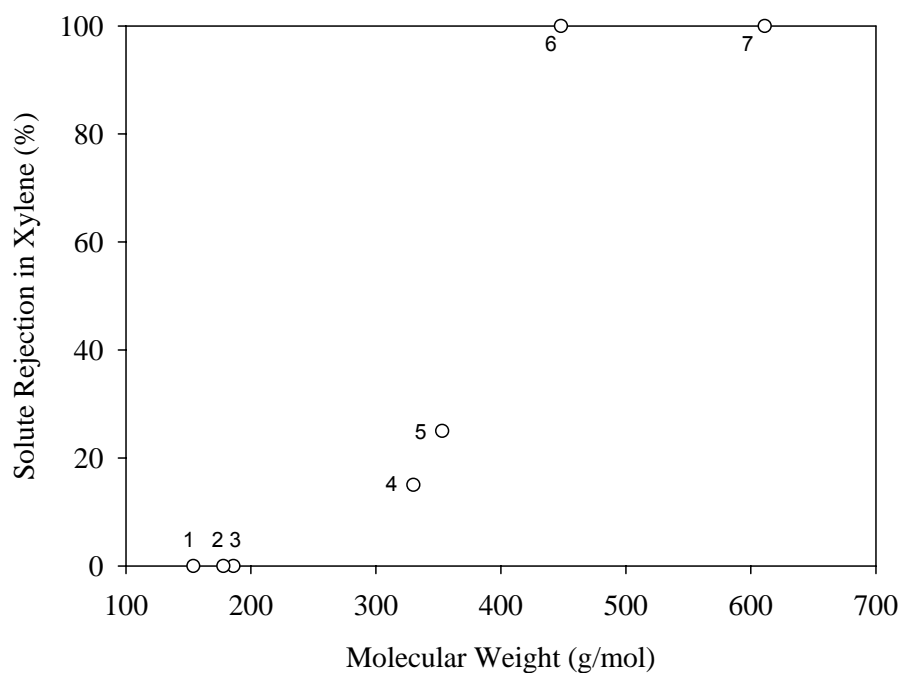


Figure 5: Rejection of low-polarity solutes in a xylene solvent. 1. Acenaphthene, 2. Anthracene, 3. Ferrocene, 4. 9,10-Diphenylanthracene, 5. Iron (III) acetylacetonate, 6. Iron (III) naphthenate, 7. Copper (II) naphthenate.

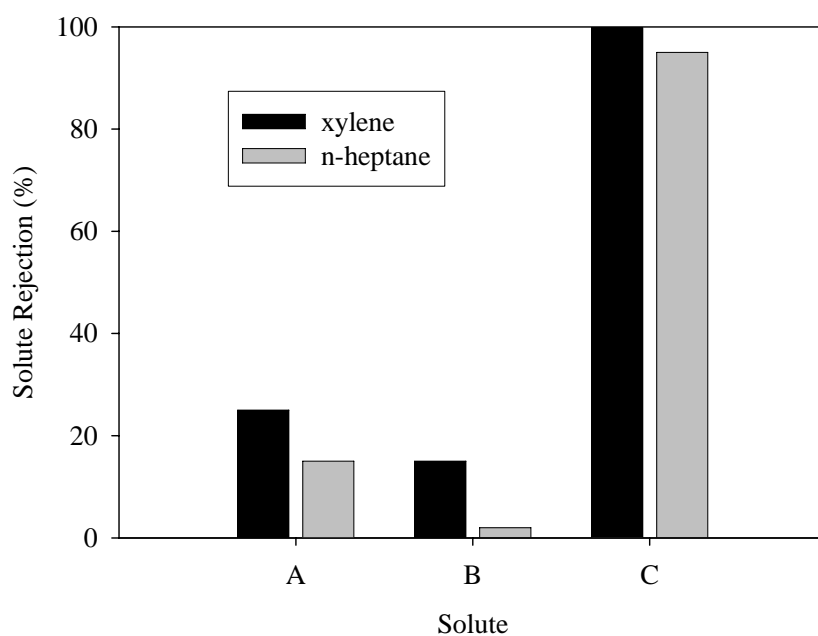


Figure 6: Rejection in xylene and n-heptane: A - Iron (III) acetylacetonate. B - 9,10-Diphenylanthracene. C - Iron (III) naphthenate.

Solvent	Gradient ($\times 10^{-2} \text{ l m}^{-2} \text{ h}^{-1} \text{ kPa}^{-1}$)	Intercept ($\text{l m}^{-2} \text{ h}^{-1}$)
n-hexane	8.41	2.53
n-heptane	7.00	2.49
i-hexane	7.80	3.17
i-heptane	6.25	2.23
i-octane	4.66	1.56
cyclohexane	3.66	1.10
xylene	4.90	1.74

Table 1: Gradients and intercepts of the flux-pressure relationship for the solvents studied.

Material	Classification	Molecular weight	Viscosity at 20°C (Pa s)	Hildebrand solubility parameter ($\text{MPa}^{0.5}$)
PDMS	polymer	-	-	15.5
n-hexane	straight chain alkane	86	0.00032	14.9
n-heptane	straight chain alkane	100	0.00039	15.3
i-hexane	branched alkane	86	0.00027	14.3
i-heptane	branched alkane	100	0.00034	14.4
i-octane	branched alkane	112	0.00046	14.6
Cyclohexane	cyclic alkane	84	0.00095	16.8
Xylene	cyclic aromatic	98	0.00065	18.2
Water	-	18	0.00114	47.5
Ethanol	alcohol	46	0.00115	26.5
Iron (III) acetylacetonate	OM	353	-	-
9,10 Diphenylanthracene	PNA	330	-	-
Ferrocene	OM	186	-	-
Anthracene	PNA	178	-	-
Acenaphthene	PNA	154	-	-
Iron (III) naphthenate	OM	467	-	-
Copper (II) naphthenate	OM	612	-	-

Table 2: Classification and properties of test materials (PNA \equiv poly-nuclear aromatic; OM \equiv organometallic).